The Journal of Engineering

The 14th IET International Conference on AC and DC Power Transmission (ACDC 2018)

IET Journals
The Institution of Engineering and Technology

Self-adaptable reactive power-voltage controller for virtual synchronous generators

eISSN 2051-3305
Received on 22nd August 2018
Accepted on 19th September 2018
E-First on 13th December 2018
doi: 10.1049/joe.2018.8452
www.ietdl.org

Bo Zhang[1,2] ✉, Dongxue Li[1], Yuke Wang[1], Xiangwu Yan[1,2]

[1]*North China Electric Power University, 619 Yonghua North Street, Baoding, People's Republic of China*

[2]*Key Laboratory of Distributed Energy Storage and Microgrid of Hebei Province, 619 Yonghua North Street, Baoding, People's Republic of China*

✉ *E-mail: adam166@163.com*

Abstract: With a higher and higher penetration of renewable energy in the grid, the principle of the virtual synchronous generator (VSG) is proposed as an attractive solution to controlling the grid-connected inverters. In common, active power-frequency and reactive power-voltage controllers play major roles in VSG control system. However, the line impedance and local loads are the critical case effecting on the control result of the two controllers. Compared with reactive power-voltage controller, active power-frequency controller is more easier to product the load sharing among the VSGs accurately. This paper presents a self-adaptable reactive power-voltage controller to deal with the sharing problem of reactive power in the parallel VSGs system, using the reactive power difference to adjust reactive power-voltage control coefficient. Then, a linearised small-signal model is established for stability analysis of the reactive power-voltage control coefficient to the parallel VSGs system. Finally, an experiment of two parallel VSGs system based on the self-adaptable reactive power-voltage controllers is performed, with different line impedance. Results obtained from the experiment verify the effectiveness of the proposed self-adaptable reactive power-voltage controllers in the parallel VSGs system.

1 Introduction

In the recent years, distributed generation (DG) has recently been considered as a promising solution to meet the increased demand for utility with smaller effects on the environment and distribution infrastructures. With the higher and higher penetration of renewable energy sources, the problem of grid steady operation is increasingly severe. With lacking inertia needed to support and participating in the frequency and voltage control of an AC system, the renewable energy sources (RESs) inverters are hence unable to contribute to the improvement of system stability [1]. This issue can be addressed through the application of the concept of virtual synchronous generator (VSG), which combine VSC and synchronous generator (SG) characteristics. The VSG control algorithm of a power electronics inverter is a control feature that can be added to a converter controller to enable it to behave as an SG [2].

The active power-frequency and reactive power-voltage controllers play a major roles in VSG control system. When VSG operates in island mode, the droop control strategy, based on the internally frequency and voltage droop, is an effective strategy to distribute power between inverters without intercommunication [3].

Based on the assumption of pure inductive lines, the traditional droop control uses the frequency to regulate the active power (P–f) and voltage to control reactive power (Q–U). But in low-voltage power system, the transmission line is mainly resistive, so the traditional droop control cannot be the same effective as in high-voltage system. Adding inductance into the transmission line or adjusting the output impedance of the inverter into inductive helps relieve the power coupling issue [4]. The real power–frequency (P–ω) and reactive power–voltage (Q–U) droop control methods have been conventionally adopted to obtain the accurate power-sharing performance with a decentralised method [5]. With resistive transmission line, the transmitted reactive power is proportional to phase angle difference and the active power is related to voltage difference, so P–U droop control was discussed in [6]. But neither P–f droop control nor P–U droop control is able to completely make power decoupling.

This paper focused on active power and reactive power-sharing performance of the parallel VSGs system, and proposed a self-adaptable reactive power-voltage controller to deal with the sharing problem of reactive power in the paralleled VSG system, using the reactive power difference to adjust reactive power-voltage control coefficient. Then a linearised small-signal model is established for stability analysis of the reactive power-voltage control coefficient to the parallel VSGs system.

2 Principle of VSG control

The VSG concept is first presented in the subject of the VSYNC project [7]. A VSG is a grid-connected or alone power electronic inverter controlled to emulate the behaviour of an energy source with a well-defined rotational inertia towards the grid during a limited period of time, thereby increasing the grid frequency stability and giving balancing algorithms, control, and protection devices more time to restore normal grid operation after a fault or contingency.

Fig. 1 shows the basic principle of VSG. The distributed energy resources (DREs) such as wind and solar energy can be equivalent to a prime motor, and a classical three-phase voltage-source PWM inverter was used as synchronous generators that can mimic the properties of SGs such as power droop, damping, and inertia. Following the principle of the VSG, every distributed grid-connected inverter operated as a synchronous generator, so that the method and theory of large-scale grid stability controlling could be transplanted into controlling a microgrid with a high penetration of DREs [8]. Therefore, the problem of the fluctuating DREs affecting the voltage and frequency of the microgrid can be solved effectively.

A general overview of the VSG control systems and the power system configuration is shown in Fig. 2. A mathematical model of VSG and its associated control loops are used to control a three-phase voltage-source inverter (VSI). The blocks composing the internal representation of the SG and its traditional droop control loops are grouped at the bottom of the figure. Here, a classical second-order model for VSG is adopted which mainly includes the electrical model and mechanical model. A simplified swing equation represented as the mechanical model can be shown as

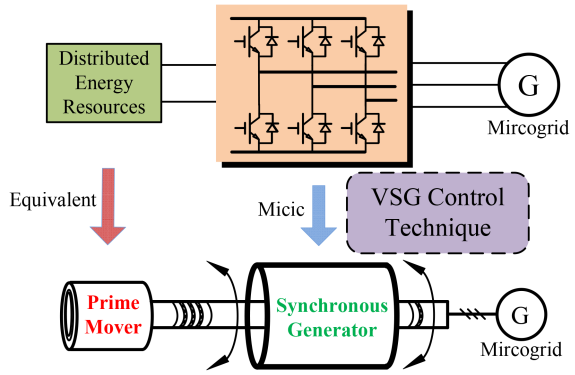

Fig. 1 *Concept of virtual synchronous generator*

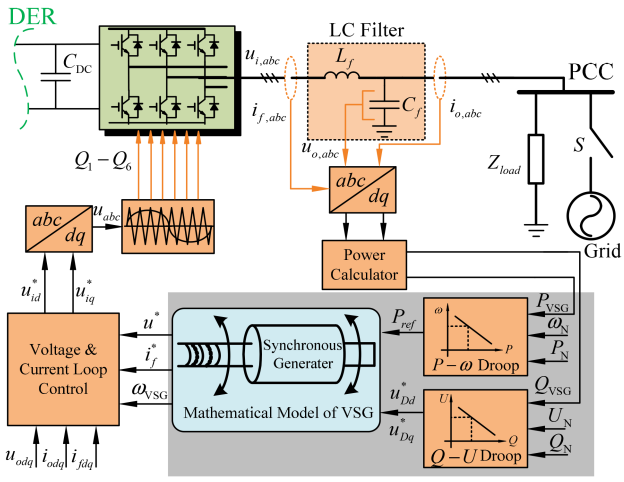

Fig. 2 *Structure of the multiple parallel VSGs system*

Equation (a). It should be noted that all the variables are indicated by physical values here.

$$\begin{cases} J\omega\dfrac{\mathrm{d}(\omega-\omega_N)}{\mathrm{d}t} = P_m - P_e - D(\omega-\omega_g) \\ \dfrac{\mathrm{d}\theta}{\mathrm{d}t} = \omega \end{cases} \tag{1}$$

where P_m and P_e are mechanical active power and electromagnetic active power, respectively, ω is the rotating speed of the generator, ω_N is the rated angular frequency, ω_g is the angular frequency of the grid, θ is electric angle, D is the damping coefficient, and J is the rotor inertia.

The electrical equation of the synchronous generator is used to represent a quasi-stationary electrical model (QSEM) by (2), assumed that the SG stator impedance is algebraic in SRRF. The variables in SRRF are translated from those in static three-phase frame by an amplitude invariant park transformation. And all the variables in SRRF equations are described by complex space-vector notation according to $\dot{X} = x_d + \mathrm{j}x_q$ [9].

$$\dot{E} = \dot{U} + \dot{I}(r_a + \mathrm{j}x_a) \tag{2}$$

where r_a is the armature resistance, x_a is the synchronous reactance, $\dot{U}$ is the output voltage of the VSG, $\dot{E}$ is the excitation electromotive force, and $\dot{I}$ is the stator current.

Based on the basic principle of SG governor and automatic voltage regulator (AVR), the distributed grid-connected inverter mimics the frequency regulator and voltage regulator of the SG with the conventional droop control such as P–f droop and Q–U droop. The droop control equations are expressed as

$$\omega = \omega_N - D_P(P - P_N) \quad (D_P > 0) \tag{3}$$

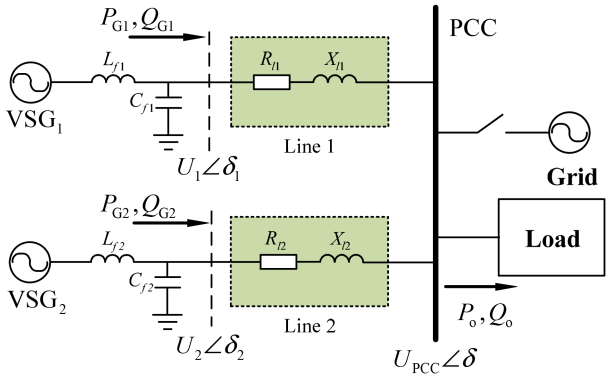

Fig. 3 *Equivalent circuit of two parallel VSGs system*

$$U = U_N - D_q(Q - Q_N) \quad (D_q > 0) \tag{4}$$

where P_N and Q_N are rated active power and reactive power, respectively. P and Q are the output active power and reactive power of VSG, and U_N is the rated voltage. D_P is damping coefficient of P–f control loop, D_q is damping coefficient of Q–U control loop.

3 Self-adaptable *Q–U* controller

In Fig. 2, it is obvious that the mathematical modelling and droop control are the core of VSG realisation. For the mathematical modelling of VSG, there is a consensus among the current literatures that the second-order model is widespread used in VSG modelling, which mainly depends on the swing equation [1]. Hence, the droop control has been focused on and discussed in this subsection.

First of all, the equivalent circuit of two parallel VSGs system is shown as Fig. 3 [10], the output active power P_i and reactive power Q_i of each VSG connected to the point of common coupling (PCC) can be written as

$$\begin{cases} P_i = \dfrac{U_iU_{\mathrm{PCC}}R_{\mathrm{li}}\cos\delta_i - U_{\mathrm{PCC}}^2R_{\mathrm{li}} + U_iU_{\mathrm{PCC}}X_{\mathrm{li}}\sin\delta_i}{R_{\mathrm{li}}^2 + X_{\mathrm{li}}^2} \\ Q_i = \dfrac{U_iU_{\mathrm{PCC}}X_{\mathrm{li}}\cos\delta_i - U_{\mathrm{PCC}}^2X_{\mathrm{li}} - U_iU_{\mathrm{PCC}}R_{\mathrm{li}}\sin\delta_i}{R_{\mathrm{li}}^2 + X_{\mathrm{li}}^2} \end{cases} \tag{5}$$

where U_i and U_{PCC} are the amplitude of the output voltage of the VSG and the PCC, respectively. δ_i is the phase angle between the output voltage of VSG and the voltage of the PCC.

In VSG control system, the P–f and Q–U droop control are often used to mimic the primacy frequency and voltage regulation properties of SG. But the control relationships of the P–f and Q–U are obtained under the assumption that the line impendence is inductive, R_{li} is neglected, and δ_i is quite small, then $\sin\delta = \delta$ and $\cos\delta = 1$. Consequently, the active power and reactive power can be expressed as

$$\begin{aligned} P_i &\approx \frac{U_{\mathrm{pcc}}U_i}{X_{\mathrm{li}}}\delta_i \\ Q_i &\approx \frac{U_{\mathrm{pcc}}}{X_{\mathrm{li}}}(U_i - U_{\mathrm{pcc}}) \end{aligned} \tag{6}$$

According to (6), by adjusting P_i and Q_i independently, frequency and amplitude of the PCC voltage are assured as shown in (3) and (4) [4, 11].

Hence, the conventional P–f and Q–U droop method has an intrinsic problem related to the line impedance. For multiple VSGs parallel operation, by only using the conventional droop method, the VSG dynamics cannot be independently controlled.

It should be noted that the frequency is a global variable, so active power load can be exactly distributed all the time. Consequently, the problem of P–f controller is not discussed here,

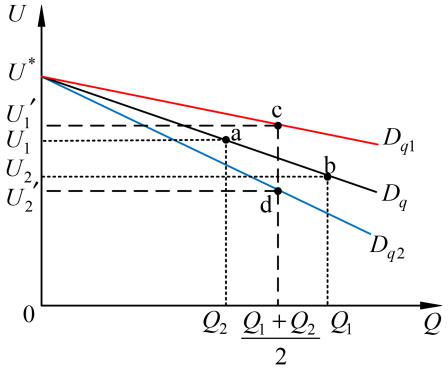

Fig. 4 *Principle of the self-adaptable Q-U controller*

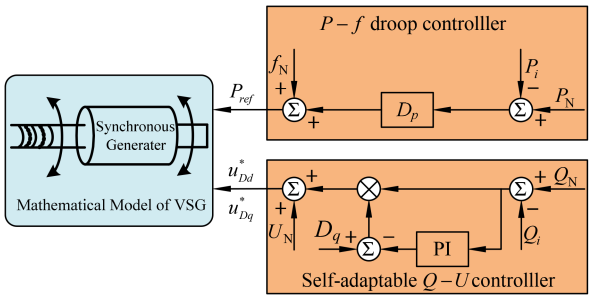

Fig. 5 *Overview of the self-adaptable Q-U controller*

as a corresponding self-adaptable Q–U controller is proposed in VSG control system to for the decoupling of active power and reactive power.

The principle of the self-adaptable Q–U control which can make the load sharing between the parallel VSGs is shown in Fig 4. Originally, the two VSGs operate at the points 'a' (U_1,Q_1) and 'b' (U_2,Q_2), the operating points 'c' and 'd' are the operating points of VSGs after using the self-adaptable Q–U controller. Since the different line impedance, the reactive power of two parallel VSGs are also different with the same droop coefficient D_p, as $Q_1 > Q_2$. It is clearly that the reactive power of two parallel VSGs are both deviated from the reference value $(Q_1 + Q_2)/2$. With the effect of the self-adaptable Q–U controller, the droop coefficient of VSG_1 is increased to D_{p1}, meanwhile, the operating point of VSG_1 changes from 'a' to 'c'. Similarly, he droop coefficient of VSG_2 is decreased to D_{p2}, meanwhile, the operating point of VSG_2 changes from 'b' to 'd'. Moreover, the load accurately sharing is obtained with the two VSGs operating at 'c' and 'd', respectively.

The diagram of the self-adaptable Q–U controller is shown in Fig. 5. The proposed self-adaptable Q–U controller is equivalent to regulate the reactive power droop coefficient automatically in the conventional droop control method. The improved droop control equation can be expressed as

$$U_i = U_N - [D_p - (K_p + K_i/s)(P_N - P_i)]P_i \tag{7}$$

where K_p and K_i are the proportional coefficient and integral coefficient of the PI controller, respectively.

Due to the integrating element in the VSG control system, the load sharing in multiple VSGs parallel systems can be carried out automatically without the measured value of line impedance. Since the droop coefficients is chosen to satisfy (7), reactive power-sharing proportional to their power ratings is (always) achieved. If the average load sharing is needed, the base value of the droop coefficients of VSGs should be set to the same value. Correspondingly, if the accurate proportional load sharing is needed, the base value of the droop coefficients of VSGs should be in inverse proportion to their power ratings [12].

4 Results and analysis

4.1 Small-signal analysis

In this section, small-signal model of two parallel VSGs system with the self-adaptable Q–U controller is built for stand-alone mode. Then, based on this model, the transition responses of active power and reactive power of VSGs during a loading deviation are shown and analysed.

A state-space model for the two parallel VSGs system as shown in Fig. 3 can be obtained as given in (2)–(9), the state-space equations of the two parallel VSGs system, which contain the electrical system, the voltage and current loop controllers, the transmission line, and LC filter, are well established and can be directly adapted from [9, 13, 14]. The equations for the filter currents, the grid side currents, and the output voltage of the VSG can be derived directly from the circuit in Fig. 2, and are not presented for simple. However, the output voltage of the self-adaptable Q–U controller can be written as

$$\begin{cases} \dfrac{\mathrm{d}\xi}{\mathrm{d}t} = Q_N - Q_i \\ U_i^* = U_N + (D_q - K_\mathrm{p})(Q_N - Q_i) - K_\mathrm{i}\xi \end{cases} \tag{8}$$

Then, the non-linear state-space equations which contains 30 state variables can be linearised around stable operating points and a linearised small-signal model of two parallel VSGs system is expressed as

$$\Delta\dot{\boldsymbol{x}}_{\mathrm{sys}} = \boldsymbol{A}_{\mathrm{sys}}\Delta\boldsymbol{x}_{\mathrm{sys}} \tag{9}$$

where (see equation below) The small-signal dynamics of the linearised small-signal model as shown in (9) were accessed by performing an eigenvalue analysis for the line impendence in the system. The parametric sweep results are shown in Figs. 6 and 7, where the ratio (R/X) varies on the range of 40–0.025 and the line length (l_{line}) varies on the range of 20–800 m. In Fig. 6, low frequency eigenpair $\lambda_{17,18}$ change from two real roots into a pair of conjugate complex roots, with oscillation frequency increasing and damping ratio reduced. When the line resistance ratio reaching 0.025, eigenpair $\lambda_{13,14}$ moves into the right half plane, and then the system exhibits instability. A similar analysis can be done in Fig. 7, there are two-pairs of complex-conjugate in the high-frequency eigenvalues λ_{3-10} move towards to the right side of the complex plane, with damping ratio increasing. For the middle-frequency eigenvalues, eigenpair $\lambda_{11,12}$ move towards to the left side of the complex plane and become to a pair of complex-conjugate at last. The eigenpair $\lambda_{13,14}$ and eigenvalue λ_{15} make a little change in their location. The low frequency eigenpair $\lambda_{17,18}$ move towards unstable region making the system more oscillatory and eventually leading to instability, with line length increasing. Vice versa, a reduction in the line length can shift the eigenvalues towards the right side of the complex plane and generate instability for values lower than 190 m.

It can be seen from the above sections, the resistive component of line impedance can support damping for the system, the low-frequency and middle-frequency eigenvalues move towards to the left side of the complex plane with the line length increasing, which make the system more steady. Moreover, high-frequency

$$\begin{aligned} \Delta\mathrm{x}_{\mathrm{sys}} = [&\Delta\omega_1; \Delta P_1; \Delta Q_1; \Delta\phi_{d1}; \Delta\phi_{q1}; \Delta\gamma_{d1}; \Delta\gamma_{q1}; \Delta i_{\mathrm{ld}1}; \Delta i_{\mathrm{lq}1}; \Delta v_{\mathrm{od}1}; \cdots \\ &\Delta v_{\mathrm{oq}1}; \Delta i_{\mathrm{od}1}; \Delta i_{\mathrm{oq}1}; \Delta\xi_1; \Delta\delta_{\mathrm{v}2}; \Delta\omega_2; \Delta P_2; \Delta Q_2; \Delta\phi_{d2}; \cdots \\ &\Delta\phi_{q2}; \Delta\gamma_{d2}; \Delta\gamma_{q2}; \Delta i_{\mathrm{ld}2}; \Delta i_{\mathrm{lq}2}; \Delta v_{\mathrm{od}2}; \Delta v_{\mathrm{oq}2}; \Delta i_{\mathrm{od}2}; \Delta i_{\mathrm{oq}2}\cdots \\ &\Delta\xi_2; \Delta i_{\mathrm{load}d}; \Delta i_{\mathrm{load}q}] \end{aligned}$$

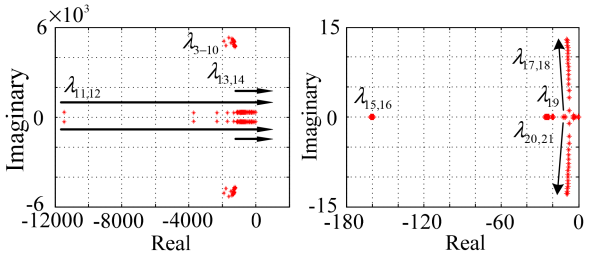

Fig. 6 *Eigenvalue loci (only the important eigenvalues shown) for a parametric sweep of the ratio of line impedance in a rage of 40 to 0.025*

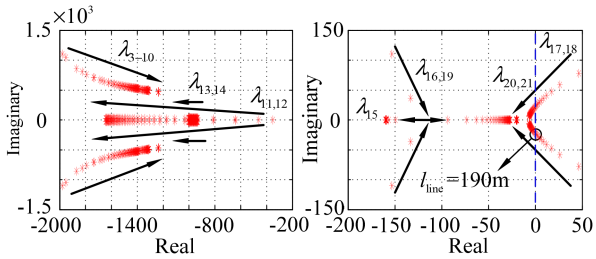

Fig. 7 *Eigenvalue loci (only the important eigenvalues shown) for a parametric sweep of the length of line in a rage of 20 to 800 m*

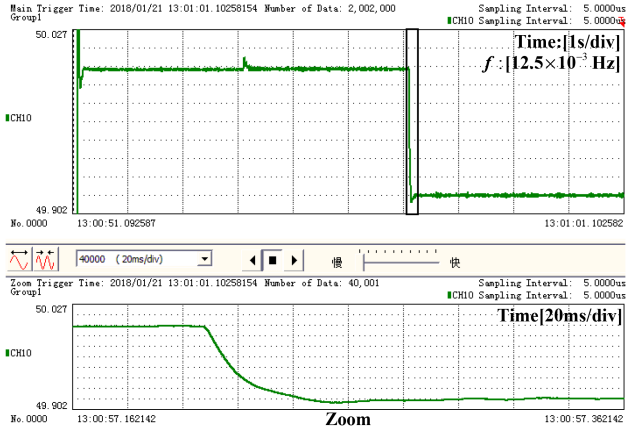

Fig. 8 *Experiment results of the system frequency*

eigenvalues are far from the imaginary axis and the corresponding movements are very little, it does not affect the system stability.

4.2 Experiment results

In an island microgrid mode, a prototype of two parallel VSGs as shown in Fig. 3 was executed and tested in the laboratory. Under laboratory conditions, the setup of the experiment system is the same as those listed in Table 1.

To verify the effectiveness of the proposed self-adaptable *Q*–*U* controller, the system is originally controlled by the conventional droop control approach with the initial load$_1$, and then VSG control method with the proposed self-adaptable *Q*–*U* controller is used at 3 s, load$_2$ is connected to PCC at 6 s as a load deviation. Figs. 8–10 show the experiment results of system frequency, active power, and reactive power, respectively. An obvious inertia delay can be observed from the system frequency in Fig. 8. And it is clear that the active power of the two VSGs can be accurate sharing, but the reactive power corresponding cannot share equally when the system is operated by the conventional droop control approach. After 3 s, an accurate power-sharing performance can be seen in both active power (5 kW) and reactive power (1.8 kvar) curves. With a load deviation at 6 s, both the active power (6.7 kW) and reactive power (2.6 kvar) sharing shown in Figs. 9 and 10 exhibit good performance.

5 Conclusion

Table 1 Experiment parameters

Parameter	Value	Parameter	Value
$S_{b1,2}$/kW	5	U_{dc}/V	700
f_{sw}/kHz	6	U_{ref}	220 V, 50 Hz
$L_{f1,2}$/mH	1	$C_{f1,2}$/μF	10
R_{line1}/Ω	0.4	L_{line1}/mH	4
R_{line2}/Ω	0.8	L_{line2}/mH	6
$D_{p1,2}$	5×10^{-5}	$D_{q1,2}$	5×10^{-3}
R_{load1}	34.9 Ω	L_{load1}	44.5 mH
R_{load2}	5.6 Ω	L_{load2}	4.47 mH
K_p	0.001	K_i	0.1

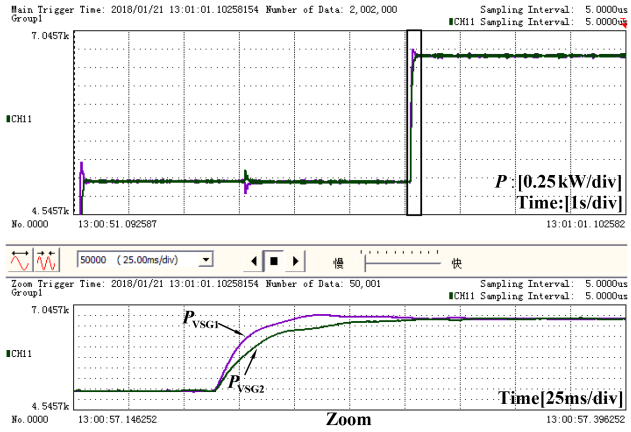

Fig. 9 *Experiment results of the active power of the two VSGs*

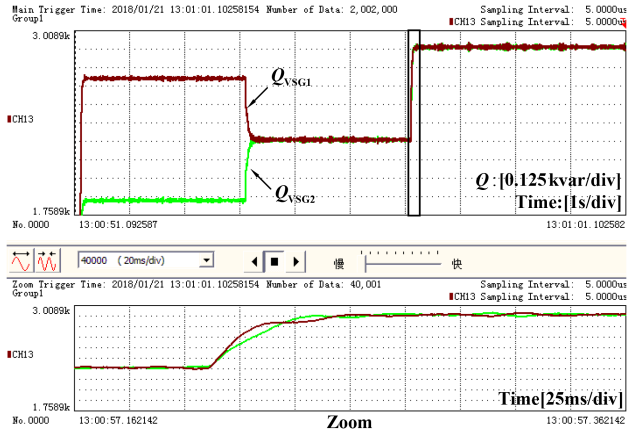

Fig. 10 *Experiment results of the reactive power of the two VSGs*

Active power-frequency and reactive power-voltage controllers play a major role in VSG control system. However, the line impedance and local loads are the critical case impacting on the control performance of the two controllers. Here, a self-adaptable reactive power-voltage controller is proposed to deal with the sharing problem of reactive power in the parallel VSGs system, which uses the reactive power difference to adjust reactive power-voltage control coefficient. For the stability analysis of the parallel VSGs system with the proposed self-adaptable reactive power-voltage controller, a linearised small-signal model is established, and the parametric sweep results of line impedance are analysed. Finally, the experimental results obtained in the laboratory are presented before drawing the final conclusions.

6 Acknowledgments

The authors would like to thank the anonymous referees for their helpful comments and suggestions. This work was supported by the Natural Science Funds of Hebei Province (Grant No. E2015502046) and the Fundamental Research Funds for the

Central Universities (Grant No. 2018MS088), in part by the Scientific Research Program of Hebei University (Grant No. Z2017132).

7 References

[1] Alsiraji, H.A., El-Shatshat, R.: 'Comprehensive assessment of virtual synchronous machine based voltage source converter controllers', *IET Gener. Transm. Distrib.*, 2017, **11**, (7), pp. 1762–1769

[2] Bevrani, H., Ise, T., Miura, Y.: 'Virtual synchronous generators: a survey and new perspectives', *Int. J. Electr. Power Energy Syst.*, 2014, **54**, (1), pp. 244–254

[3] Chandorkar, M.C., Divan, D.M., Adapa, R.: 'Control of parallel connected inverters in standalone AC supply systems', *IEEE Trans. Ind. Appl.*, 1993, **29**, (1), pp. 136–143

[4] Li, Y.W., Kao, C.N.: 'An accurate power control strategy for power-electronics-interfaced distributed generation units operating in a low-voltage multibus microgrid', *IEEE Trans. Power Electron.*, 2009, **24**, (12), pp. 2977–2988

[5] Vasquez, J., Mastromauro, R., Guerrero, J.M.*, et al.*: 'Voltage support provided by a droop-controlled multifunctional inverter', *IEEE Trans. Ind. Electron.*, 2009, **56**, (11), pp. 4510–4519

[6] Guerrero, J.M., Jose, M., Garcia de Vicuña, L.*, et al.*: 'Decentralized control for parallel operation of distributed generation inverter using resistive output impedance', *IEEE Trans. Ind. Electron.*, 2007, **54**, (2), pp. 994–1004

[7] Driesen, J., Visscher, K.: 'Virtual synchronous generators'. Proc. Int. Conf. Conversion and Delivery of Electrical Energy in the 21st Century, Pittsburgh, PA, USA, July 2008, pp. 1–3

[8] Kroutikova, N., Hernandez-Aramburo, C.A., Green, T.C.: 'State-space model of grid-connected inverters under current control mode', *IET Electr. Power Appl.*, 2007, **1**, (3), pp. 29–338

[9] Mo, O., D'Arco, S., Suul, J.A.: 'Evaluation of virtual synchronous machines with dynamic or quasi-stationary machine models', *IEEE Trans. Ind. Electron.*, 2016, **64**, (7), pp. 5952–5962

[10] Brabandere, K.D., Bolsens, B., Keybus, J.V.D.*, et al.*: 'A voltage and frequency droop control method for parallel inverters', *IEEE Trans. Power Electron.*, 2007, **22**, (4), pp. 1107–1115

[11] Li, Y., Vilathgamuwa, D.M., Loh, P.C.: 'Design, analysis, and real-time testing of a controller for multibus microgrid system', *IEEE Trans. Power Electron.*, 2004, **19**, (5), pp. 1195–1204

[12] Zhong, Q.C.: 'Robust droop controller for accurate proportional load sharing among inverters operated in parallel', *IEEE Trans. Ind. Electron.*, 2012, **60**, (4), pp. 1281–1290

[13] Rasheduzzaman, M., Mueller, J.A., Kimball, J.W.: 'An accurate small-signal model of inverter- dominated islanded microgrids using dq reference frame', *IEEE J. Emerg. Sel. Top. Power Electron.*, 2017, **2**, (4), pp. 1070–1080

[14] Liu, J., Miura, Y., Ise, T.: 'Comparison of dynamic characteristics between virtual synchronous generator and droop control in inverter-based distributed generators', *IEEE Trans. Power Electron.*, 2015, **31**, (5), pp. 3600–3611